Maejo Int. J. Sci. Technol. **2021**, *15*(03), 302-314

Maejo International Journal of Science and Technology

ISSN 1905-7873
Available online at www.mijst.mju.ac.th

Technical Note

Degradation of 3,5-dichlorobiphenyl catalysed by copper salen complexes and their graphene oxide immobilised counterparts

Cong-Jie Dai [1] and Xue-Fei Zhou [1, 2, *]

[1] Fujian Province Key Laboratory for the Development of Bioactive Material from Marine Algae, Quanzhou Normal University, Quanzhou, 362000, China
[2] Faculty of Chemical Engineering, Kunming University of Science and Technology, Kunming, 650500, China
* Corresponding author, e-mail: lgdx602@sina.com

Received: 29 May 2021 / Accepted: 26 December 2021 / Published: 30 December 2021

Abstract: Cu([H_4]salen) prepared from Cu([H_2]salen) was immobilised on graphene oxide (GO) to obtain Cu([H_4]salen)/GO. The presence of the complex on GO was verified by X-ray diffraction, Fourier transform infrared spectroscopy and Raman spectroscopy. Cu([H_4]salen)/GO exhibits better catalytic capacity as compared to Cu([H_2]salen), Cu([H_4]salen) and Cu([H_2]salen)/GO in the degradation of 3,5-dichlorobiphenyl. The reaction conditions were optimised based on the removal of 3,5-dichlorobiphenyl. Cu([H_4]salen)/GO also shows good performance in total carbon content conversion and ecotoxicity removal compared with other catalysts.

Keywords: graphene oxide, degradation of 3,5-dichlorobiphenyl, biomimetic catalysis, copper salen complex, immobilised salen complex

INTRODUCTION

Persistent organic pollutants are those organic compounds of anthropogenic origin with features of persistence, toxicity, bio-accumulation and long-range environmental transport. Generally, they are divided into three categories: (1) pesticides (e.g. aldrinand toxaphene), (2) unintentionally produced by-products (e.g. polychlorinated dibenzo-p-dioxins), and (3) industrial chemicals (e.g. polychlorinated biphenyls (PCBs)) [1, 2]. PCBs have been demonstrated to cause a variety of adverse health effects on living beings and human beings such as neurotoxicity and dermatological diseases [3]. They are highly stable and highly resistant to chemical, photolytic and biological degradation. Conventional treatments commonly used to treat PCB-contaminated water

Maejo Int. J. Sci. Technol. **2021**, *15*(03), 302-314

are inadequate to convert PCBs to less harmful or non-toxic compounds. Therefore, it is necessary to study new process to treat PCB [4].

In the past decades a variety of strategies have been applied to treating PCBs. Khammar et al. [5] synthesised magnetic nanoparticles functionalised with β-cyclodextrin and used it to treat high concentrations of PCBs in oil. A maximum PCBs removal of 82% was attained under optimum conditions. Huang et al. [6] studied the photolysis of polychlorinated biphenyls in different media. It was shown that photodegradation rates were faster in methanol/water than in n-hexane. Quiroga et al. [7] reported results of direct treatment of PCBs sorbed to glass beads and sand using the direct Fenton oxidation and desorption combined with the photo-Fenton process**.** The results displayed 98% removal of the original PCB structure and 82% dechlorination within a reaction time of 72 hr, and the level of congener chlorination affected the degree of removal. An electrochemical remediation technology was assessed in field to evaluate its potential for treating PCB-contaminated sediment under anaerobic conditions. The final results indicated that a greater than 90% reduction in total PCBs was obtained relative to the the control [8]. In addition, the incorporation of reductive catalysis and thermal degradation has been shown to contribute effectively toward dechlorination of polychlorinated aromatics [9]. Furthermore, biotreatment, reported to be active in catalysed degradation of PCBs, could take place through anaerobic dechlorination, aerobic microbial degradation, and a combination of both. However, the applications of biodegradation are only confined to mild reaction conditions such as low temperature and low pH and still result in low efficiency [10, 11].

Salen complexes provide an alternative solution for the degradation of PCBs as it combines enzymatic and chemical process in a single catalyst via the biomimetic route [12, 13]. Due to this synergistic effect , the use of salen complexes has therefore been widely studied in oxidation reactions, reduction of ketones, polymerisation, ring-opening of epoxides, allylic alkylation, etc. [14]. In oxidation reactions, the selectivity and efficiency of substrate conversion are dramatically enhanced with Schiff base metal salen complexes [15]. Moreover, their catalytic performances can be improved by hydrogenation of C=N to C-N [16]. Some studies revealed that hydrogenated salen ligands with saturated secondary and tertiary amines showed higher chemical stability and binding affinities towards the substrate than the prototype Schiff base salen ligand [17, 18]. The immobilisation of metal salen complexes allows them to be more robust catalysts with high stability. In particular, many materials may be used as supports for immobilising the catalysts, including natural minerals, adsorbents, glasses and organics [19]. Among them, graphene oxide (GO) is an excellent support. It affords high chemical stability and high specific surface area.

Qian et al. [20] successfully developed a GO-based copper salen complex to activate persulfate for removal of triclosan in aqueous solution. In Mahmoodi and Saffar-Dastgerdi's study [21], laccase was immobilised on the nanoparticles of GO to degrade Direct Red 23. The effects of GO ratio, catalyst dosage, dye concentration and pH on Direct Red 23 degradation were evaluated. The catalyst showed good reusability over five cycles, high storage stability and thermal stability. Lin et al. [22] reported that incorporating reduced GO in TiO_2 photocatalyst could enhance photocatalytic degradation of carbamazepine, ibuprofen and sulfamethoxazole in aqueous solutions. Yek et al. [23] synthesised a GO-nanosheet-immobilised copper(II) complex. The catalytic performance of the nanocatalyst was evaluated with 4-nitrophenol, Rhodamine B, methylene blue, nigrosin and congo red. The surface nature of the GO nanosheet changed after immobilisation of the complex, causing an effective increase in the catalytic prowess. PdO/SiO_2/GO composite was prepared to degrade thiophene, benzothiophene and dibenzothiophene [24]. The performance of

Maejo Int. J. Sci. Technol. **2021**, *15*(03), 302-314

$PdO/SiO_2/GO$ composite was better than that of PdO/SiO_2. This was attributed to the assumption that incorporation of GO increased the specific surface area and the Pd incorporation rate. In the present study the catalytic effect on 3,5-dichlorobiphenyl oxidation in aqueous solution was investigated, in which copper salen complexes and their GO-immobilised counterparts were employed as biomimetic catalysts.

MATERIALS AND METHODS

Chemicals

Chloroform (Sinopharm Chemical Reagent Co., China) was dried with $NaHCO_3$ and $CaCl_2$, and distilled prior to use. 3,5-Dichlorobiphenyl (chromatographic grade) was purchased from Sigma-Aldrich and stored at 4 °C. GO (99.0 %) was purchased from Sinopharm Chemical Reagent Co. (China). All other chemicals (Sinopharm Chemical Reagent Co., China) were of analytical grade and used without further purification, whereas Milli-Q-Plus ultrapure water was used in all experiments.

Because 3,5-dichlorobiphenyl is hydrophobic substance, it cannot be directly dissolved in water. A stock solution of 100 mg/L was thus prepared by dissolving 3,5-dichlorobiphenyl in acetone.

Preparation of Catalysts

The reactions used for the preparation of catalysts are shown in Scheme 1 [25]. Firstly, [H_2]salen and [H_4]salen ligands were prepared. Salicylaldehyde (0.02 mol) was dissolved in ethanol (50 mL) followed by the addition of ethanol solution (25 mL) containing ethylenediamine (0.01 mol). Under stirring, the mixture was refluxed for 2 hr. After cooling, yellow crystals were filtered out, washed with petroleum ether, and recrystallised in ethanol to obtain [H_2]salen (yield: 72.5%). [H_2]salen (0.01 mol) was dissolved in methanol (60 mL) and sodium borohydride (0.011 mol) was added into the solution. The mixture was stirred at room temperature for 2 hr. The solvent was removed by vacuum distillation. The crude product was washed with water and recrystallised in ethanol to obtain [H_4]salen (yield: 77.3%). [H_2]salen: ^{1}H-NMR (Bruker DRX spectrometer, 300 MHz, $CDCl_3$, TMS, δ ppm) 13.21 (2H, s, OH), 8.36 (2H, s, CH=N), 7.30-6.81 (8H, m, Ar-H), 3.92 (4H, s, N-CH_2CH_2-N); FTIR (Nicolet Impact 410 spectrometer, KBr pellet, cm^{-1}) 3420 (OH), 3052 (C=C), 2924, 2892 (Aliph-H), 2730-2585 (H-bonding), 1636 (C=N), 1600, 1498, 1452 (Ph); elemental analysis ($C_{16}H_{16}N_2O_2$) (Vario EL Elemental Analyzer 1106, data in brackets are theoretical values) 71.35% C (71.64%), 5.72% H (5.97%), 10.37% N (10.44%), 11.63% O (11.94%). [H_4]salen: ^{1}H-NMR (Bruker DRX spectrometer, 300 MHz, $CDCl_3$, TMS, δ ppm) 7.24-6.77 (8H, m, Ar-H), 3.98 (4H, s, N-CH_2CH_2-N), 2.85 (4H, s, N-CH_2); FTIR (Nicolet Impact 410 spectrometer, KBr pellet, cm^{-1}) 3285 (N-H), 3034 (C=C), 2912, 2855 (Aliph-H), 2705-2565 (H-bonding), 1600, 1465 (Ph); elemental analysis ($C_{16}H_{20}N_2O_2$) (Vario EL Elemental Analyzer 1106, data in brackets are theoretical values) 70.37% C (70.58%), 7.58% H (7.35%), 10.41% N (10.29%), 11.62% O (11.76%).

Secondly, Cu([H_2]salen) and Cu([H_4]salen) were prepared. [H_2]salen or [H_4]salen (1.18 g) was dissolved in ethanol (60 mL) and copper acetate (1.1 g) was added. The mixture was refluxed for 1 hr. The resulting mixture was then filtered. The solid was washed with water and recrystallised in chloroform/petroleum ether to obtain Cu[H_2]salen or Cu([H_4]salen). Cu([H_2]salen): $CuC_{16}H_{14}N_2O_2$, 19.06% Cu (19.27%), 58.51% C (58.27%), 4.07% H (4.24%), 8.54% N (8.49%),

Maejo Int. J. Sci. Technol. **2021**, *15*(03), 302-314

9.28% O (9.71%). Cu([H_4]salen): $CuC_{16}H_{18}N_2O_2$, 19.26% Cu (19.04%), 57.38% C (57.57%), 5.53% H (5.39%), 8.47% N (8.39%), 9.27% O (9.59%).

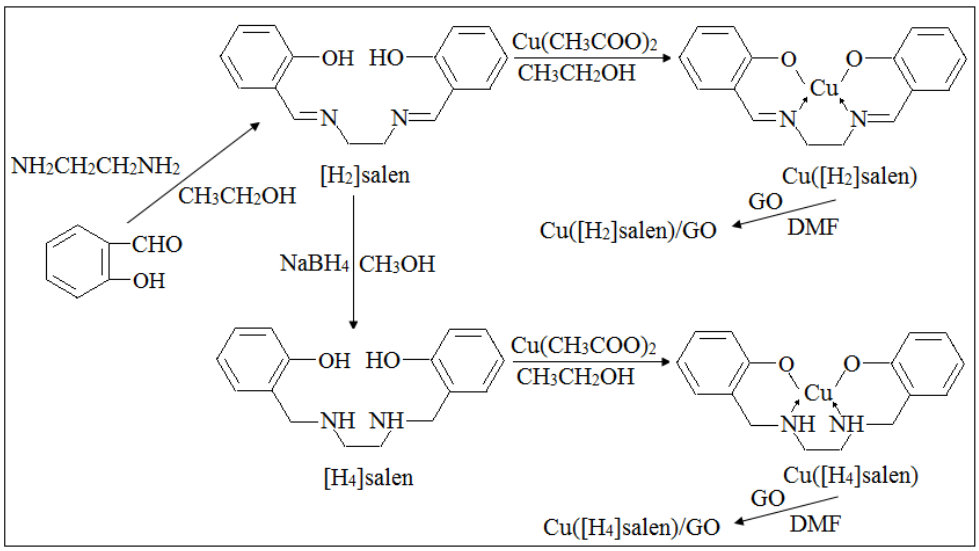

Scheme 1. Synthesis of Cu([H_2]salen) and Cu([H_4]salen) and their immobilisation on GO [25]

The GO-immobilised Cu([H_2]salen) and Cu([H_4]salen) were synthesised according to the reported method [23]. Briefly, Cu([H_2]salen) or Cu([H_4]salen) (0.03 g) was thoroughly dispersed in N, N-dimethylformamide (15 mL) by ultrasonication. GO (15 g, in 600 mL water)) was added to the mixture, which was then treated under ultrasonic conditions for 5 hr at 30 °C. After that the mixture was filtered and the obtained solid was washed with water and dried at 50 °C under reduced pressure. The resulting GO-immobilised Cu([H_2]salen) and Cu([H_4]salen) were denoted Cu([H_2]salen)/GO and Cu([H_4]salen)/GO respectively. Their loading capacities of Cu([H_2]salen)/GO and Cu([H_4]salen)/GO were ~0.6 g/mg based on the copper analysis with atomic absorption spectrometry (Shimadzu AA-6800). The specific surface areas of Cu([H_2]salen)/GO and Cu([H_4]salen)/GO were analysed with Brunauer-Emmett-Teller equation with a Micromeritics ASAP-2020 surface area analyzer (USA). Their X-ray diffraction (XRD) patterns were recorded on a Rigaku Dmax X-ray diffractometer (Ni-filtered, Cu Kα radiation, 40 kV and 30 mA, 2θ, 5-40°, scanning speed 6°/min.). FTIR spectra were obtained in the range of 400-4000 cm^{-1} on a Nicolet Impact 410 spectrometer. Raman spectra analysis was carried out at a laser excitation wavelength of 530 nm on confocal micro-Raman spectrometer (Almega XR).

Degradation of 3,5-Dichlorobiphenyl

The degradation of 3,5-dichlorobiphenyl by hydrogen peroxide was carried out in a flask immersed in a water bath using Cu([H_2]salen), Cu([H_4]salen), Cu([H_2]salen)/GO or Cu([H_4]salen)/GO as catalyst. For comparison, a control trial was also carried out under identical conditions in the absence of catalyst. The initial pH of the system was adjusted with buffer solution to examine the effect of pH on the catalytic reaction. The mixture was stirred at 120 r/min. and 0.50 mL aliquots were collected. The samples were subsequently extracted using solid phase extraction which was also used to clean and pre-concentrate the 3,5-dichlorobiphenyl analyte in the water samples using an LC-C18 column. The solid phase extraction was conditioned with methanol [26].

Maejo Int. J. Sci. Technol. **2021**, *15*(03), 302-314

The 3,5-dichlorobiphenyl was determined by HPLC (Shimadzu SZP-10) equipped with Zorbax Eclipse Plus C18 column (250 mm×4.6 mm×5 μm). The mobile phase was methanol/water mixture (4:1 v/v) and the flow rate of the mobile phase was 1.0 mL/min. The total carbon content (TCC) of the solutions was determined with an elemental analyser (Vario EL Elemental Analyzer 1106). TCC conversion is then calculated:

$$TCC\ conversion = \frac{TCC_0 - TCC_t}{TCC_0} \times 100\ \%$$

where TCC_0 is TCC of the solution before treatment and TCC_t is TCC of the solution after treatment. The toxicity of the solutions was determined according to the Microtox Acute Toxicity Test with Microtox Model 500 Toxicity Analyzer (SDI Co., USA) using a freeze-dried preparation of marine bacterium *Vibrio fischeri* (*Photobacterium phosphoreum*) (Sigma-Aldrich) [27].

RESULTS AND DISCUSSION

Characterisation of Materials

Results of specific surface area analysis of prepared Cu([H_2]salen)/GO and Cu([H_4]salen)/GO show that their specific surface areas, 562.7 m^2/g and 548.2 m^2/g respectively, are lower than that of GO (587.5 m^2/g). This may partly confirm the catalysts' successful introduction into the GO structure [28].

XRD patterns of GO, Cu([H_2]salen)/GO and Cu([H_4]salen)/GO are shown in Figure 1. The peak at 10.5° corresponds to oxygen-containing groups such as carboxyl, hydroxyl and epoxy groups between the graphite layers [29]. The characteristic peak arising from the linkage between oxygen-containing groups of GO and Cu([H_2]salen) or Cu([H_4]salen) is ascertained at 25.7°, which further confirms a successful immobilisation of Cu([H_2]salen) and Cu([H_4]salen) on GO [30]. In addition, unaltered XRD patterns of Cu([H_2]salen)/GO and Cu([H_4]salen)/GO compared to GO indicate that the GO structure was not destroyed during the immobilisation process [31].

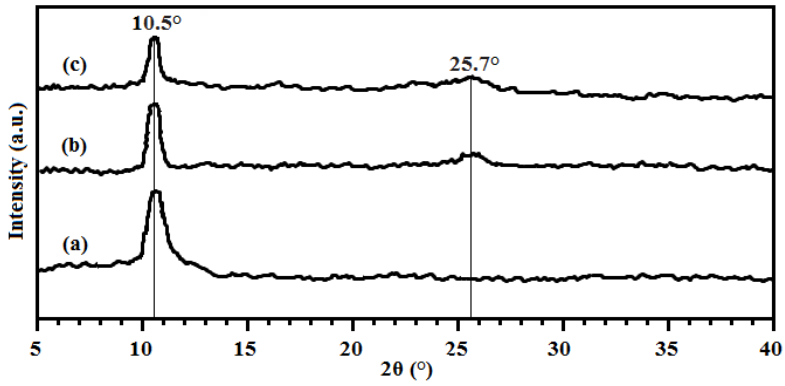

Figure 1. XRD spectra of (a) GO, (b) Cu([H_2]salen)/GO and (c) Cu([H_4]salen)/GO

The FTIR spectra of GO, Cu([H_2]salen)/GO and Cu([H_4]salen)/GO are shown in Figure 2. After the immobilisation of the complexes on GO, there is a change in the characteristic IR peaks of the constituting units. Notably the peak at 3200 cm^{-1} (Figure 2c) corresponds to the N-H bond, which ascertains a reduced state from C=N of Cu([H_2]salen) (1660 cm^{-1}) to C-N of Cu([H_4]salen) (1330 cm^{-1}) [32]. For Cu([H_2]salen)/GO (Figure 2b) and Cu([H_4]salen)/GO (Figure 2c), Si-O-Si and Si-O-C peaks are found at 1105 cm^{-1} and 1020 cm^{-1} respectively. They occur due to linkage

Maejo Int. J. Sci. Technol. **2021**, *15*(03), 302-314

between the complex and GO [33]. Characteristic peaks at 568 cm^{-1} and 470 cm^{-1} correspond to the vibration of Cu-N and Cu-O respectively [25]. These peaks indicate that Cu([H_2]salen) and Cu([H_4]salen) have been immobilised on GO successfully.

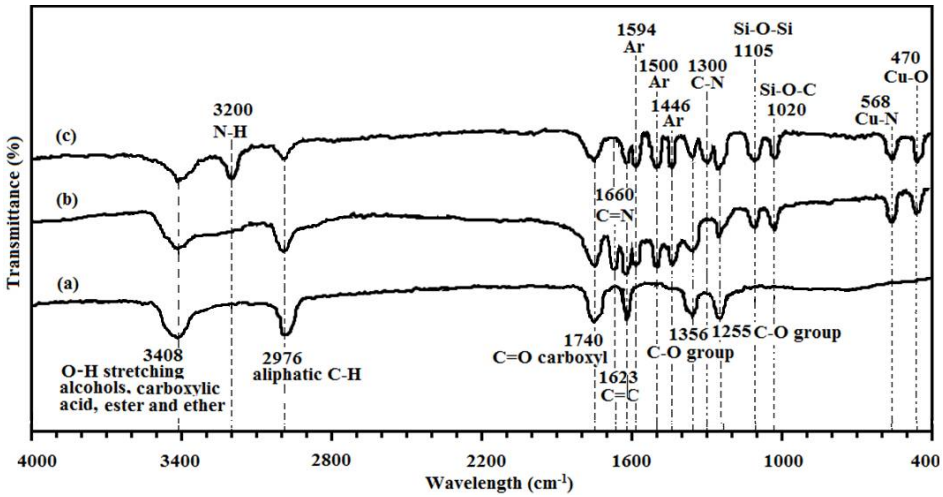

Figure 2. FTIR spectra of (a) GO, (b) Cu([H_2]salen)/GO and (c) Cu([H_4]salen)/GO

Similar XRD and FTIR results are reported by Zhou [25] for zeolite-encapsulated Cu([H_2]salen) and Cu([H_4]salen). After Cu([H_2]salen) and Cu([H_4]salen) were encapsulated into zeolite, XRD peaks at 9.7°, 11.5° and 14.8° were structurally unaltered. The appearance of the bands at 568 cm^{-1} (Cu-N), 470 cm^{-1} (Cu-O), 1500 cm^{-1} (aromatic ring), 1500-1300 cm^{-1} (C-N for [H_4]salen) provided a further conclusive evidence of the successful encapsulation of Cu([H_4]salen) and Cu([H_2]salen) into the zeolite. In another study [34] $MPSC_6$ binuclear biomimetic complexes (Figure 3) were immobilised on GO. The diffraction peaks at around 10.6° of GO-immobilised $MPSC_6$ complexes did not disappear, indicating that the structure of GO was not destroyed after immobilisation of these complexes on the GO; the immobilised complexes showed a broad peak at 25.5°. Further, the FTIR spectra showed some characteristic peaks such as 3200 cm^{-1} (GO-OH), 1720 cm^{-1} (GO-C=O), 1623 cm^{-1} (GO-C=C), 1400 cm^{-1} (GO-CH), 1048 cm^{-1} (GO-CO), 1105 cm^{-1} (Si-O-Si), 1020 cm^{-1} (Si-O-C), 1597 cm^{-1} (salen C=N), 529 cm^{-1} (M-N, M=Co, Cu, Zn, Ni) and 430 cm^{-1} (M-O).

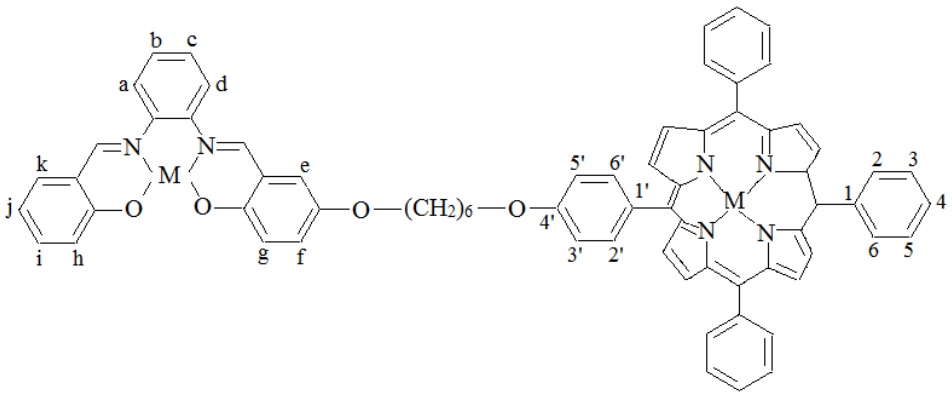

MPTPP-$(CH_2)_6$-salenM($MPSC_6$), M=Co, Cu, Zn and Ni

Figure 3. Structure of $MPSC_6$ complexes (MPTPP = metal 5,10,15-triphenyl-20-mesohydroxylphenylporphyrin) [34]

Maejo Int. J. Sci. Technol. **2021**, *15*(03), 302-314

Figure 4 shows the Raman spectra of GO, Cu([H_2]salen)/GO and Cu([H_4]salen)/GO. Two characteristic peaks are observed for GO at 1320 cm^{-1} and 1595cm^{-1} [35]. The peaks observed in all of the samples are similar. Another characteristic feature is that Cu([H_2]salen)/GO and Cu([H_4]salen)/GO exhibit broaden D band compared to GO, while the position of G band varies between samples: that of Cu([H_2]salen)/GO and Cu([H_4]salen)/GO shifts from 1595 cm^{-1} to 1608 cm^{-1}. These findings show that the immobilisation results in bonding via oxygen-containing groups between GO and the complex [36].

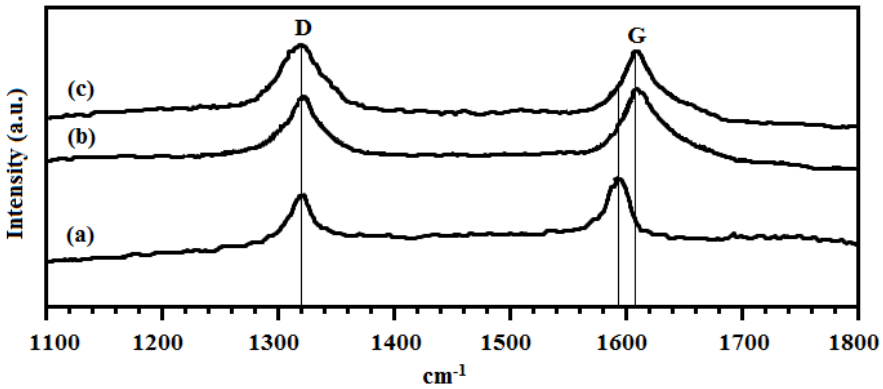

Figure 4. Raman spectra of (a) GO, (b) Cu([H_2]salen)/GO and (c) Cu([H_4]salen)/GO

Catalytic Capacity of Copper Salen Complexes and Their Effects

In order to evaluate the immobilisation and hydrogenation of Cu([H_2]salen) and their effects on catalytic performance, 3,5-dichlorobiphenyl was used as substrate in catalytic degradation by H_2O_2 using both Cu([H_2]salen) and Cu([H_4]salen) complexes and their GO-immobilised analogues as catalysts. As shown in Figure 5, the degradation rates of 3,5-dichlorobiphenyl by the GO-immobilised complexes (Cu([H_2]salen)/GO and Cu([H_4]salen)/GO) are higher than those by Cu([H_2]salen) and Cu([H_4]salen). The porous structure of GO affords a uniform dispersion of the active species and accessible voids for the substrate to approach the immobilised complex. The GO promotes the binding of 3,5-dichlorobiphenyl molecules onto its surface and offers maximum interactions with the complex [37]. Moreover, the [H_4] complexes, both unimmobilised and immobilised, are more active than the corresponding [H_2] complexes in the degradation of 3,5-dichlorobiphenyl. For example, after reaction for 60 min., Cu([H_2]salen) gives 36.3% removal and Cu([H_2]salen)/GO provides 46.2% removal, while Cu([H_4]salen) gives 41.8% removal and Cu([H_4]salen)/GO gives 51.3% removal. The results show that hydrogenation of C=N bond of Cu([H_2]salen) to flexible C-N bond contributes to the catalytic enhancement [38]. Thus, our attention was focused on further optimisation of 3,5-dichlorobiphenyl oxidation by Cu([H_4]salen)/GO.

Maejo Int. J. Sci. Technol. **2021**, *15*(03), 302-314

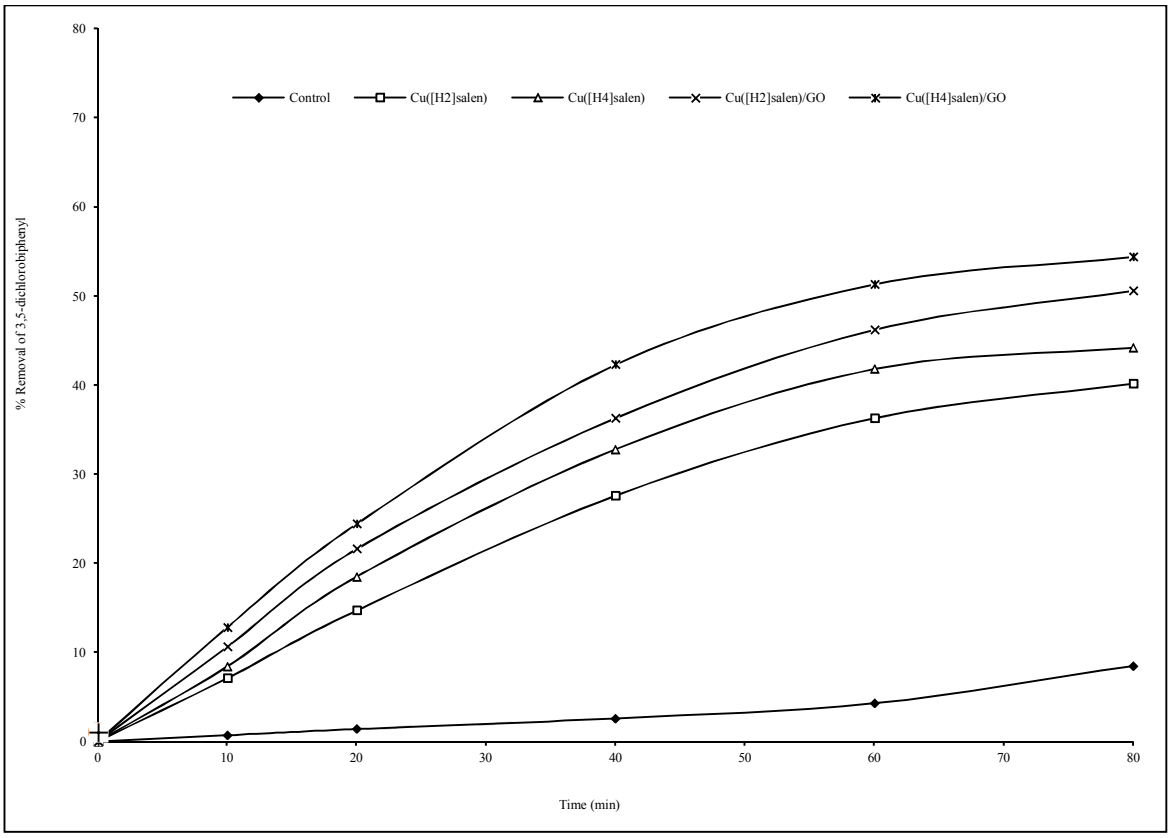

Figure 5. Catalytic degradation of 3,5-dichlorobiphenyl. [3,5-dichlorobiphenyl]=0.04 mmol/L, [catalyst]=2 ppm, pH=7.0, [H_2O_2]=0.40 mmol/L, *T*=30 °C

As can be seen from Figure 6a, the degradation of 3,5-dichlorobiphenyl increases with increasing Cu([H_4]salen)/GO concentration. The more Cu([H_4]salen)/GO is used, the more active sites are available for H_2O_2 to degrade 3,5-dichlorobiphenyl [39]. As seen from the results, a relatively low concentration (4 ppm) of Cu([H_4]salen)/GO, displays satisfactory degradation of 3,5-dichlorobiphenyl.

The effects of temperature and H_2O_2 concentration on 3,5-dichlorobiphenyl degradation are similar (Figures 6b, 6c) and are more or less as expected [44]. The effect of pH is shown in Figure 6d; the 3,5-dichlorobiphenyl removal efficiency is highest at pH 8 (96.2%) and sharply drops under strong acidic and alkali conditions. The pH seems to affect the intramolecular structure of salen, and weak alkaline solution may favour the equilibrium between mononuclear and binuclear complexes towards the catalytically more active species [41].

The catalysis effects were further comparatively assessed by ecotoxicity and TCC conversion conducted on the treated solutions and the results are presented in Figure 7. After the organic pollutant is degraded, carbon dioxide is released as mineralisation; TCC thus decreases and TCC conversion increases. The higher the TTC conversion, the more pollutant is degraded by mineralisation [42, 43]. It was found as shown in Figure 7 that the ecotoxicity values of all treated solutions are lower than that of the control. Especially, the Cu([H_4]salen)/GO affords the most positive effect compared to the other catalysts, and the corresponding ecotoxicity of the solution is lowest and the TCC conversion of the solution is highest. This can be explained by the fact that 3,5-dichlorobiphenyl is mostly degraded by the catalyst and more carbon dioxide is released, so the TCC conversion is consequently high. As more non-toxic compounds are formed, the ecotoxicity is

Maejo Int. J. Sci. Technol. **2021**, *15*(03), 302-314

correspondingly low [44]. Biomimetic catalysis promotes the formation of phenoxy radicals resulting in the degradation of refractory linkages between benzene rings [45].

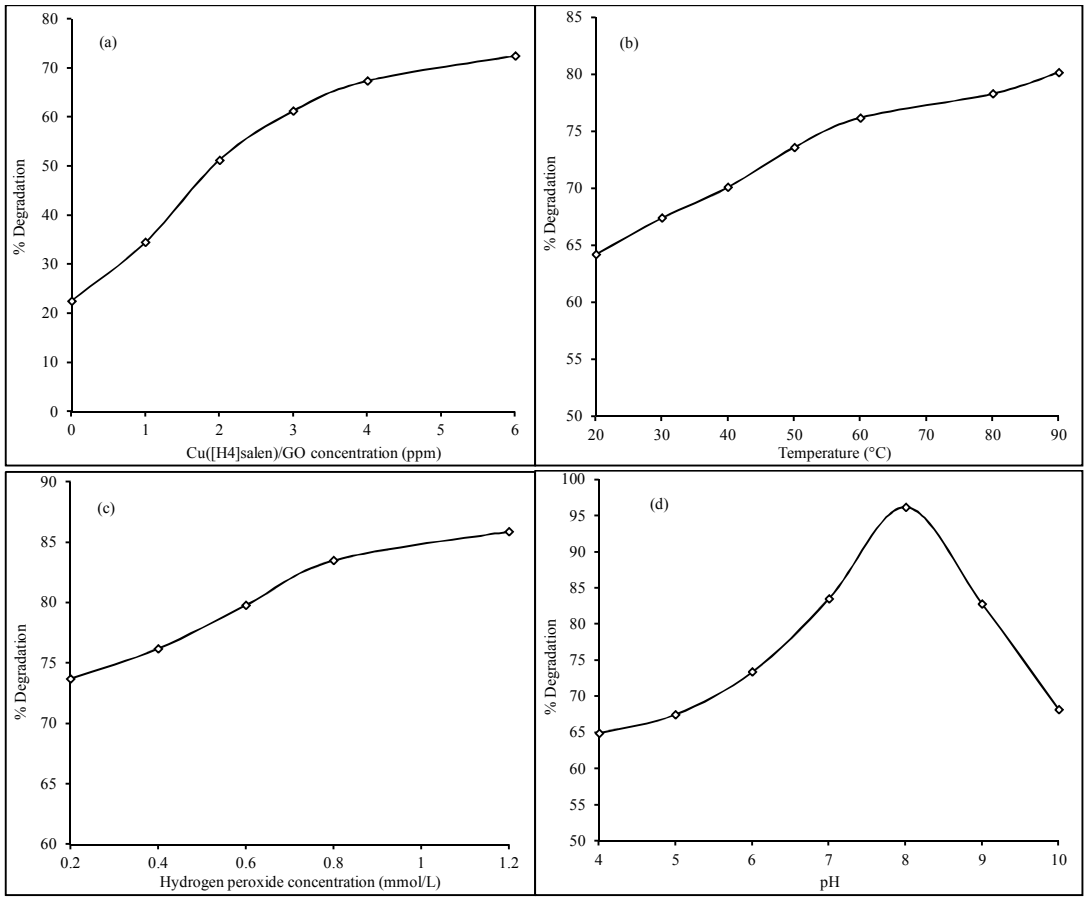

Figure 6. Catalytic degradation of 3,5-dichlorobiphenyl using Cu([H_4]salen)/GO as catalyst: (a) effect of Cu([H_4]salen)/GO concentration ([3,5-dichlorobiphenyl]=0.04 mmol/L, pH=7.0, [H_2O_2]=0.40 mmol/L, *T*=30 °C, *t*=60 min.); (b) effect of reaction temperature ([3,5-dichlorobiphenyl]=0.04 mmol/L, [Cu([H_4]salen)/GO]=4 ppm, pH=7.0, [H_2O_2]=0.40 mmol/L, *t*=60 min.); (c) effect of hydrogen peroxide concentration ([3,5-dichlorobiphenyl]=0.04 mmol/L, [Cu([H_4]salen)/GO]=4 ppm, pH=7.0, *T*=60 °C, *t*=60 min.); (d) effect of pH value ([3,5-dichlorobiphenyl]=0.04 mmol/L, [Cu([H_4]salen)/GO]=4 ppm, [H_2O_2]=0.8 mmol/L, *T*=60 °C, *t*=60 min.)

Maejo Int. J. Sci. Technol. **2021**, *15*(03), 302-314

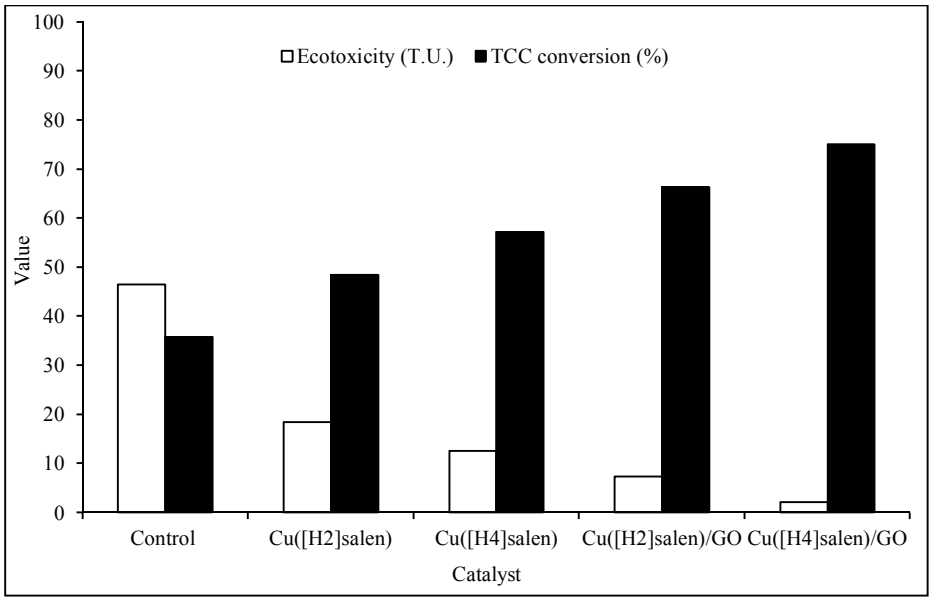

Figure 7. Effects of catalytic treatment on ecotoxicity and TCC of treated solutions: [3,5-dichlorobiphenyl]=0.04 mmol/L, [Cu([H_4]salen)/GO]=4 ppm, [H_2O_2]=0.80 mmol/L, T=60 °C, t =60 min. (T.U.= toxic unit)

CONCLUSIONS

Based on our results, the GO-supported Cu([H_4]salen) complex has the potential for improving 3,5-dichlorobiphenyl oxidation. The results could be useful for a chemical approach to the pollutant management. However, additional experiments on improving the activity of the complex against refractory pollutants as well as the detailed mechanism of the complex in promoting degradation are needed in order to make commercial uses of this complex in the future.

ACKNOWLEDGEMENTS

This work was supported by the Open Research Foundation of Fujian Province Key Laboratory for the Development of Bioactive Material from Marine Algae of Quanzhou Normal University (2020FZSK02).

REFERENCES

1. L. S. Filippos, S. Taniguchi, P. Baldassin, T. Pires and R. C. Montone, "Persistent organic pollutants in plasma and stable isotopes in red blood cells of *Caretta caretta*, *Chelonia mydas* and *Lepidochelys olivacea* sea turtles that nest in Brazil", *Mar. Pollut. Bull.*, **2021,** *167*, Art.no.112283 (DOI: 10.1016/j.marpolbul.2021.112283).
2. C. Driesen, M. Zennegg, I. Morel, H. D. Hess, B. Nowack and S. Lerch, "Average transfer factors are not enough: The influence of growing cattle physiology on the transfer rate of polychlorinated biphenyls from feed to adipose", *Chemosphere*, **2021**, *270*, Art.no.129698 (DOI: 10.1016/j.chemosphere.2021.129698).
3. D. E. Vlotman, J. C. Ngila, T. Ndlovu, B. Doyle, E. Carleschi and S. P. Malinga, "Hyperbranched polymer membrane for catalytic degradation of polychlorinated biphenyl-153 (PCB-153) in water", *React. Funct. Polym.*, **2019**, *136*, 44-57.
4. B. Sun, Q. Li, M. Zheng, G. Su, S. Lin, M. Wu, C. Li, Q. Wang, Y. Tao, L. Dai, Y. Qin and B. Meng, "Recent advances in the removal of persistent organic pollutants (POPs) using

multifunctional materials: A review", *Environ. Pollut.*, **2020**, *265*, Art.no.114908 (DOI: 10.1016/j.envpol.2020.114908).

5. S. Khammar, N. Bahramifar and H. Younesi, "Optimization using the response surface methodology for adsorption of polychlorinated biphenyls (PCBs) from transformer oil by magnetic CMCD-Fe_3O_4@SiO_2 nanoparticles", *Mater. Chem. Phys.*, **2020**, *252*, Art.no.123195 (DOI: 10.1016/j.matchemphys.2020.123195).
6. C. Huang, Y. Zeng, X. Luo, Z. Ren, Y. Tian and B. Mai, "Comprehensive exploration of the ultraviolet degradation of polychlorinated biphenyls in different media", *Sci. Total Environ.*, **2021**, *755*, Art.no.142590 (DOI: 10.1016/j.scitotenv.2020.142590).
7. J. M. Quiroga, A. Riaza and M. A. Manzano, "Chemical degradation of PCB in the contaminated soils slurry: Direct Fenton oxidation and desorption combined with the photo-Fenton process", *J. Environ. Sci. Health A.*, **2009**, *44*, 1120-1126.
8. L. M. Zanko, J. K. Wittle and S. Pamukcu, "Case study: Electrochemical geo-oxidation (ECGO) treatment of Massachusetts New Bedford Harbor sediment PCBs", *Electrochim. Acta*, **2020**, *354*, Art.no.136690 (DOI: 10.1016/j.electacta.2020.136690).
9. A. Perosa, M. Selva and T. Maschmeyer, "Multiphase hydrodechlorination of polychlorinated aromatics – Towards scale-up", *Chemosphere*, **2017**, *173*, 535-541**.**
10. C. M. Bako, T. E. Mattes, R. F. Marek, K. C. Hornbuckle and J. L. Schnoor, "Biodegradation of PCB congeners by Paraburkholderia xenovorans LB400 in presence and absence of sediment during lab bioreactor experiments", *Environ. Pollut.*, **2021**, *271*, Art.no.116364 (DOI: 10.1016/j.envpol.2020.116364).
11. Y. Xiang, Z. Y. Xing, J. Liu, W. Qin and X. Huang, "Recent advances in the biodegradation of polychlorinated biphenyls", *World J. Microb. Biotechnol.*, **2020**, *36*, Art.no.145 (DOI: 10.1007/s11274-020-02922-2).
12. V. J. Mayani, S. V. Mayani and S. W. Kim, "A sustainable nanocomposite Au(salen)@CC for catalytic degradation of eosin Y and chromotrope 2R dyes", *Sci. Rep.*, **2017**, *7*, Art.no.7239 (DOI: 10.1038/s41598-017-07707-6).
13. S. A. Kuznetsova, I. V. Gorodishch, A. S. Gak, V. V. Zherebtsova, I. S. Gerasimov, M. G. Medvedev, D. K. Kitaeva, E. A. Khakina, M. North and Y. N. Belokon, "Chiral titanium(IV) and vanadium(V) salen complexes as catalysts for carbon dioxide and epoxide coupling reactions", *Tetrahedron,* **2021,** *82*, Art.no.131929 (DOI: 10.1016/j.tet.2021.131929).
14. J. Min, Z. H. Xia, T. C. Zhang, H. Y. Su, Y. F. Zhi and S. Y. Shan, "Recent development of magnetic nanomaterial-supported M(salen) composites as recyclable heterogeneous catalysts", *Chem. Pap.*, **2021**, *75*, 2965-2980.
15. K. C. Gupta and A. K. Sutar, "Catalytic activities of Schiff base transition metal complexes", *Coord. Chem. Rev.*, **2008**, *252*, 1420-1450.
16. R. I. Kureshy, A. Das, N. H. Khan, S. H. R. Abdi and H. C. Bajaj, "Cu(II)-macrocylic [H_4]salen catalyzed asymmetric nitroaldol reaction and its application in the synthesis of α1-adrenergic receptor agonist (R)-phenylephrine", *ACS Catal.*, **2011**, *1*, 1529-1535.
17. X. Zhao, D. Zhang, R. Yu, S. S. Chen and D. H. Zhao, "Tetrahydrosalen uranyl (VI) complexes: Crystal structures and solution binding study", *Eur. J. Inorg. Chem.*, **2018**, *2018*, 1185-1191.
18. M. Quiroz-Guzman, A. G. Oliver, A. J. Loza and S. N. Brown, "Redox-active tetrahydrosalen (salan) complexes of titanium", *Dalton Trans.*, **2011**, *40*, 11458-11468.
19. M. Niakan, Z. Asadi and M. Masteri-Farahani, "Immobilization of salen molybdenum complex on dendrimer functionalized magnetic nanoparticles and its catalytic activity for the

epoxidation of olefins", *Appl. Surf. Sci.*, **2019**, *481*, 394-403.
20. L. Qian, P. Liu, S. Shao, M. Wang, X. Zhan and S. Gao, "An efficient graphene supported copper salen catalyst for the activation of persulfate to remove chlorophenols in aqueous solution", *Chem. Eng. J.*, **2019**, *360*, 54-63.
21. N. M. Mahmoodi and M. H. Saffar-Dastgerdi, "Clean laccase immobilized nanobiocatalysts (graphene oxide - zeolite nanocomposites): From production to detailed biocatalytic degradation of organic pollutant", *Appl. Catal. B. Environ.*, **2020**, *268*, Art.no.118443 (DOI: 10.1016/j.apcatb.2019.118443).
22. L. Lin, H. Y. Wang, W. B. Jiang, A. R. Mkaouar and P. Xu, "Comparison study on photocatalytic oxidation of pharmaceuticals by TiO_2-Fe and TiO_2-reduced graphene oxide nanocomposites immobilized on optical fibers", *J. Hazard. Mater.*, **2017**, *333*, 162-168.
23. S. M. G. Yek, D. Azarifar, M. Nasrollahzadeh, M. Bagherzadeh and M. Shokouhimehr, "Heterogenized Cu(II) complex of 5-aminotetrazole immobilized on graphene oxide nanosheets as an efficient catalyst for treating environmental contaminants", *Sep. Purif. Technol.*, **2020**, *247*, Art.no.116952 (DOI: 10.1016/j.seppur.2020.116952).
24. J. C. Xu, B. Zhang, Y. K. Lu, L. G. Wang, W. Y. Tao, X. Teng, W. S. Ning and Z. K. Zhang, "Adsorption desulfurization performance of PdO/SiO_2@graphene oxide hybrid aerogel: Influence of graphene oxide", *J. Hazard. Mater.*, **2022**, *421*, Art.no.126680 (DOI: 10.1016/j.jhazmat.2021.126680).
25. X. F. Zhou, "Application of zeolite-encapsulated Cu(II) [H_4]salen derived from [H_2]salen in oxidative delignification of pulp", *RSC Adv.*, **2014**, *4*, 28029-28035.
26. L. M. Madikizela, S. F. Muthwa and L. Chimuka, "Determination of triclosan and ketoprofen in river water and wastewater by solid phase extraction and high performance liquid chromatography", *S. Afr. J. Chem.*, **2014**, *67*, 143-150.
27. B. Thongrom, P. Amornpitoksuk, S. Suwanboon and J. Baltrusaitis, "Photocatalytic degradation of dye by Ag/ZnO prepared by reduction of Tollen's reagent and the ecotoxicity of degraded products", *Korean J. Chem. Eng.*, **2014**, *31*, 587-592.
28. G. Sharma, A. Kumar, M. Naushad, S. Sharma, A. A. Ghfar, T. Ahamad, C. Si and F. J. Stadler, "Graphene oxide supported La/Co/Ni trimetallic nano-scale systems for photocatalytic remediation of 2-chlorophenol", *J. Mol. Liq.*, **2019**, 294, Art.no.111605 (DOI: 10.1016/j.molliq.2019.111605).
29. N. Mehrabi, H. Q. Lin and N. Aich, "Deep eutectic solvent functionalized graphene oxide nanofiltration membranes with superior water permeance and dye desalination performance", *Chem. Eng. J.*, **2021**, *412*, Art.no.128577 (DOI: 10.1016/j.cej.2021.128577).
30. Z. Ghadamyari, A. Khojastehnezhad, S. M. Seyedi, F. Taghavi and A. Shiri, "Graphene oxide functionalized Zn(II) salen complex: An efficient and new route for the synthesis of 1,2,3-triazole derivatives", *Chemistryselect*, **2020**, *5*, 10233-10242.
31. M. Ghabdian, M. A. Nasseri, A. Allahresani and A. Motavallizadehkakhky, "Heterogenized Cu (II) salen complex grafted on graphene oxide nanosheets as a precursing catalyst for the Pd-free Sonogashira coupling", *Appl. Organomet. Chem.*, **2018**, 32, Art.no.e4545 (DOI: 10.1002/aoc.4545).
32. P. H. Aubert, P. Audebert, P. Capdevielle, M. Maumy and M. Roche, "Electrochemical oxidative polymerization of binuclear 'anil' and 'salen'-type complexes and tetrahydro derivatives", *New J. Chem.*, **1999**, *23*, 297-301.
33. I. Parra, S. Valbuena and F. Racedo, "Measurement of non-linear optical properties in graphene

oxide using the Z-scan technique", *Spectrochim. Acta A*, **2021**, *244*, Art.no.118833 (DOI:10.1016/j.saa.2020.118833).

34. X.-F. Zhou, Z.-R. Zou and X.-J. Yang, "MPSC6 binuclear complexes immobilized on graphene oxide for oxidation of lignin model compounds and lignin", *Rev. Roumaine. Chim.*, **2020**, *65*, 973-982.
35. A. Y. Lee, K. Yang, N. D. Anh, C. Park, S. M. Lee, T. G. Lee and M. S. Jeong, "Raman study of D* band in graphene oxide and its correlation with reduction", *Appl. Surf. Sci.*, **2021**, *536*, Art.no.147990 (DOI: 10.1016/j.apsusc.2020.147990).
36. N. Chadha, R. Sharma and P. Saini, "A new insight into the structural modulation of graphene oxide upon chemical reduction probed by Raman spectroscopy and X-ray diffraction", *Carbon Lett.*, **2021**, *31*, 1125-1131.
37. Y. Wang, S. S. Li, H. Y. Yang and J. Luo, "Progress in the functional modification of graphene/graphene oxide: a review", *RSC Adv.*, **2020**, *10*, 15328-15345.
38. S. Akine, T. Taniguchi, W. K. Dong, S. Masubuchi and T. Nabeshima, "Oxime-based salen-type tetradentate ligands with high stability against imine metathesis reaction", *J. Org. Chem.*, **2005**, *70*, 1704-1711.
39. H. Oshita, T. Suzuki, K. Kawashima, H. Abe, F. Tani, S. Mori, T. Yajima and Y. Shimazaki, "Pi-pi stacking interaction in an oxidized Cu^{II}-salen complex with a side-chain indole ring: An approach to the function of the tryptophan in the active site of galactose oxidase", *Chem. Eur. J.*, **2019**, *25*, 7649-7658.
40. M. A. Aramendia, V. Borau, I. M. Garcia, C. Jimenez, F. Lafont, A. Marinas, J. M. Marinas and F. J. Urbano, "Influence of the reaction conditions and catalytic properties on the liquid-phase hydrodechlorination of chlorobenzene over palladium-supported catalysts: Activity and deactivation", *J. Cat.*, **1999**, *187*, 392-399.
41. J. H. Cheng, F. Gou, X. H. Zhang, G. Y. Shen, X. G. Zhou and H. F. Xiang, "A Class of multiresponsive colorimetric and fluorescent pH probes via three different reaction mechanisms of salen complexes: A selective and accurate pH measurement", *Inorg. Chem.*, **2016**, *55*, 9221-9229.
42. N. Stojicic, C. Baumstark-Khan, C. E. Hellweg, H. H. Grotheer, G. Reitz, W. Kolanus and R. Hemmersbach, "Toxicity of ethylene combustion condensates is directly proportional to their carbon content", *Toxicol.*, **2010**, *269*, 35-40.
43. T. X. H. Le, M. G. Cowan, M. Drobek, M. Bechelany, A. Julbe and M. Cretin, "Fe-nanoporous carbon derived from MIL-53(Fe): A heterogeneous catalyst for mineralization of organic pollutants", *Nanomater.*, **2019**, *9.* Art.no.641 (DOI: 10.3390/nano9040641).
44. W. Q., Wang, M. Chen, D. B. Wang, M. Yan and Z. F. Liu, "Different activation methods in sulfate radical-based oxidation for organic pollutants degradation: Catalytic mechanism and toxicity assessment of degradation intermediates", *Sci. Total Environ.*, **2021**, *772*, Art.no.145522 (DOI: 10.1016/j.scitotenv.2021.145522).
45. X.-F. Zhou, "A one-pot catalysis combining laccase with Cu(salen) for selective removal of refractory lignin units during oxygen delignification of bamboo kraft pulp", *Sci. For.*, **2020**, *48*, Art.no.e3393 (DOI: 10.18671/scifor.v48n127.19).